International Journal of Heat and Technology
Vol. 41, No. 5, October, 2023, pp. 1187-1194
Journal homepage: http://iieta.org/journals/ijht

Effects of Synthetic Atmosphere and Strain Rate on NO Emission from a Biogas/Hydrogen Mixture in MILD Combustion

Hadef Amar[1,2*], Mameri Abdelbaki[1,2], Aouachria Zeroual[3]

[1] Mechanical Engineering Department, SASF, University Larbi Ben M'Hidi, Oum El Bouaghi 04000, Algeria
[2] CMASMTF Laboratory, University Larbi Ben M'Hidi, Oum El Bouaghi 04000, Algeria
[3] Applied Energy Physics Laboratory (AEPL), Faculty of Material Sciences, University Batna1, Batna 05000, Algeria

Corresponding Author Email: hadef.amar@univ-oeb.dz

https://doi.org/10.18280/ijht.410509

Received: 11 February 2023
Revised: 17 June 2023
Accepted: 2 July 2023
Available online: 31 October 2023

Keywords:
biogas/hydrogen mixture, flame relative temperature, MILD combustion, NO emission, CO_2 chemical effect

ABSTRACT

This study analyzes the structure and emission of a biogas-hydrogen diffusion flame in a synthetic atmosphere composed by oxygen, nitrogen and carbon dioxide in a flameless regime. Particular attention is paid to the oxygen content in the oxidizer and the chemical effect of CO_2 on the flame structure. The study is carried out in a laminar counter flow configuration over a wide range of strain rates. Detailed chemistry (GRI 3.0 mechanism) and complex thermal and transport properties are adopted in the calculations. The results obtained indicate that the structure of the flame, temperature and species, is very sensitive to the composition and to the amount of oxygen in the oxidizer stream. Pollutant species such as NO are reduced by a combination of decreased O_2 content and increased CO_2 volumes in the oxidant stream. The CO_2 chemical effect is present as long as the O_2 concentration is greater than 3% for the whole strain rate range. This effect leads to a decrease in temperature peaks, OH and NO.

1. INTRODUCTION

The degradation of animal remains and organic matter by microorganisms under anaerobic conditions (in the absence of oxygen) generates gases. The latter is called biogas, it is mainly characterized by its chemical composition and by the resulting physical characteristics. It consists of a mixture of methane (CH_4) and carbon dioxide (CO_2).

Combustion is the state-of-the-art pathway for energy production; however, the major drawback of this technology is emissions which have a harmful effect on human health and environment [1]. Environment protection regulations are more and more constraining. They are particularly pushing to use alternative fuels and unconventional combustion modes. In order to overcome these issues of conventional combustion, two complementary research orientations have been identified, namely the utilisation of renewable fuels such as biogas [2-4] and MILD combustion mode [5]. In this mode, the flame is not visible; it is stable with uniform properties with very low emissions such as CO and NO. The MILD regime is obtained by the dilution of the fuel and oxidant jets with a strong recirculation of the combustion gases before the reaction so that the concentration of oxygen becomes very low [6]. Biogas, despite its renewable nature, has a low calorific value. Previous investigations have shown that it is possible to improve its combustion characteristics by adopting simultaneously H_2 enrichment and O_2 dilution which is required in MILD regime. Few researches on combustion in MILD mode of biogas enriched by hydrogen have been conducted. Moreover, the structures and emissions of these flames, over a wide range of H_2 concentration and operating conditions are not well understood yet.

In the following, the most recent contributions on biogas-hydrogen blended flames in conventional and MILD regimes with synthetic atmosphere are reviewed. In an opposed jets configuration of CH_4 /air, Park et al. [7] have numerically studied the effect of the air dilution by H_2O, CO_2 and N_2 on the flame structure and NO emission. Detailed chemistry is adopted and heat loss by radiation at low strain rate was considered. It is found that the maximum flame temperature reduction was important when dilution is operated by CO_2 followed by H_2O and then N_2. Despite of the high heat capacity of H_2O, the reduction of the flame temperature is due to thermal effect of CO_2; whereas, in the case of H_2O addition the reduction results from chemical effect. In an experimental study Zhen et al. [8] considered the flame stability of a biogas enriched by hydrogen with addition of CO_2 and N_2. The authors found that hydrogen addition stabilize the flame; also, the increase of CO_2 in biogas reduces the temperature and soot more efficiently than N_2. The impacts of scalar dissipation, volume of hydrogen and carbon dioxide in the biogas, on the characteristics of the flame and its emissions have been taken into account by Mameri and Tabet [9]. The opposed jet configuration is adopted at atmospheric pressure. The authors proved that CO_2 augmentation reduces flame temperature and NO emission. The flameless combustion regime approves the importance of the preheating of air flow by combustion products such as CO_2 and H_2O, which plays the role of a diluent by their physico-chemical properties [10, 11]

Few works examined the biogas enriched by hydrogen in MILD regime, Chen et al. [12] demonstrated the effects of air preheating, composition of oxidizer and hydrogen volume in the fuel mixture on the biogas flame structure. Latice-Boltzman method was used in an opposed jet diffusion flame in MILD regime. For the low oxygen concentration, the temperature and emissions are significantly reduced whereas

they are all increased with hydrogen addition to the fuel [13].

Diluents in gaseous mixtures can act on the reduction of the reaction rate by decreasing the concentration of the reactants in the reaction zone for a pure dilution [14]. Also, they can change flame temperature and heat transfer between gases and flame, by their thermal effect [15]. Furthermore, diluents can decrease the concentration of reactive radicals such as OH and CH in the flame in an active dilution or chemical effect [16]. Dilution by H_2O is handled in a numerical study by Hadef et al. [17], the authors considered the MILD combustion of biogas (75% CH_4+25% CO_2) in an opposed jet diffusion flame. The hydrogen and water vapor are added to fuel side. It is noticed that species CO, NO, CO_2 and C_2H_2 are all reduced by H_2O; whereas, the hydrogen addition increases soot precursor C_2H_2. The NO formation in MILD regime is also studies by Shua et al. [18], preheated air is respectively diluted by N_2, H_2O and CO_2. The chemical and physical effects of these species on the emissions reduction are elucidated.

The objective of this study is the numerical simulation of the structure of the diffusion flame emissions of hydrogen and biogas mixture (BG75-H_2). Synthetic atmosphere was considered under several operating conditions with emphasis on the effect CO_2 chemistry. The investigation is performed in counter-flow laminar diffusion flame configuration at ambient pressure. The operating conditions considered are the following: O_2 percentage from 0 to 9%, CO_2 from 12% to 78% and the strain rate from 200 to 600 s^{-1}. The chemical effects of CO_2 are determined by the insertion instead of CO_2, an inert artificial species [16], which has the same properties as CO_2.The manuscript is organized into four sections; A brief explanation of the modeling and a detailed description of the simulation are presented in the first two sections. The results are then presented and interpreted in the third section; the last section presents the conclusion.

2. GEOMETRY CONFIGURATION, MATHEMATICAL FORMULATION AND CALCULATION STRATEGY

Figure 1 shows the geometry of a counter-current laminar diffusion flame. The first jet at the lower part injects a mixture of biogas and hydrogen while the second jet at the upper part feeds a preheated oxidant composed with a low content of O_2, N_2 and CO_2. The two jets impact and thus form a stagnation plane in a position that depends on the momentum ratio of the two jets. In this configuration, the diffusion flame takes the form of a flat sheet established near the stoichiometric composition plane, which permits the analyze by a one-dimensional model.

Table 1 summarizes operating condition, namely: composition of the synthetic atmosphere and reactants injection velocities. The relation between strain rate and reactants velocities and compositions is given by [19]:

$$a = \frac{2(-u_O)}{L}\left[1 + \frac{u_F}{(-u_O)}\sqrt{\frac{\rho_F}{\rho_O}}\right] \quad (1)$$

where, u and ρ denote velocity and density respectively, subscripts "O" and "F" refer to oxidizer and fuel flows. The distance between the two injectors is L=1.4 cm, the ambient pressure is 1 atm, and oxidizer injection temperature 1200 K. The mathematical model uses governing equations of the combustion phenomena, in the configuration of opposed jets, the equations are given by Lutz et al. [20].

$$\frac{\partial(\rho u)}{\partial x} = 0 \quad (2)$$

$$H - 2\frac{d}{dx}\left(\frac{FG}{\rho}\right) + \frac{nG^2}{\rho} + \frac{d}{dx}\left[\mu\frac{d}{dx}\left(\frac{G}{\rho}\right)\right] = 0 \quad (3)$$

$$\rho\, u\frac{dT}{dx} - \frac{1}{c_p}\frac{d}{dx}\left(\lambda\frac{dT}{dx}\right) + \frac{\rho}{c_p}\sum_k c_{p_k} V_k Y_k \frac{dT}{dx} + \frac{1}{c_p}\sum_k h_k \dot{\omega}_k - \frac{\dot{q}_r}{c_p} = 0 \quad (4)$$

$$\rho u\frac{dY_k}{dx} + \frac{d}{dx}(\rho Y_k V_k) - \dot{\omega}_k W_k = 0 \quad (5)$$

where, $G = -\rho v/r$, $F = \rho u$ and $H = (1/r)(\partial p/\partial r)$. Cp is the specific heat capacity and λ the coefficient of thermal conductivity. The species k in the mixture has a mass fraction Y_k, a diffusion velocity V_k, a specific enthalpy h_k, and a molecular mass W_k.

The flames studied fit into the optically thin model (OTM), where the radiating species are CO, CO_2, CH_4 and H_2O, and the losses per unit volume are expressed by [21]:

$$\dot{q}_r = -4\,\sigma\,K_P(T^4 - T_\infty^4) \quad (6)$$

Table 1. Oxidizer stream composition

Constant Total Volumetric Oxidizer Flow							
3% O_2							
% CO_2	18	28	38	48	58	68	78
% N_2	79	69	59	49	39	29	19
Ratio CO_2/N_2	0.23	0.41	0.64	0.98	1.49	2.34	4.11
T	1200 K	1200 K	1200 K	1200 K	1200 K	1200 K	1200 K
6% O_2							
% CO_2	15	25	35	45	55	65	75
% N_2	79	69	59	49	39	29	19
Ratio CO_2/N_2	0.19	0.36	0.59	0.92	1.41	2.24	3.95
T	1200 K	1200 K	1200 K	1200 K	1200 K	1200 K	1200 K
9% O_2							
% CO_2	12	22	32	42	52	62	72
% N_2	79	69	59	49	39	29	19
Ratio CO_2/N_2	0.15	0.32	0.54	0.86	1.33	2.14	3.79
T	1200 K	1200 K	1200 K	1200 K	1200 K	1200 K	1200 K

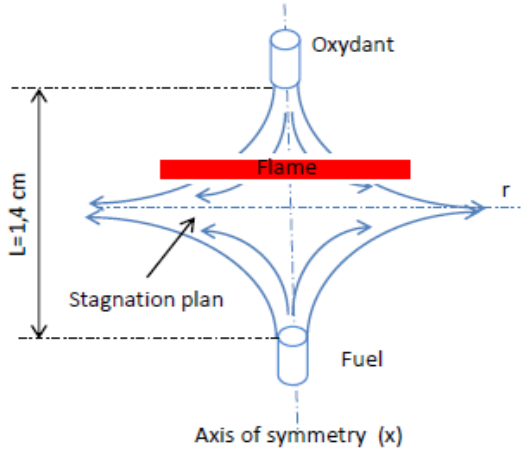

Figure 1. Opposed flow geometry, x indicates the axial direction, and r the radical one

In this equation, KP is the average absorption coefficient, it is computed in function of the species concerned by radiation (CO_2, H_2O, CO and CH_4) by:

$$K_P = P_{CO2}K_{CO2} + P_{H2O}K_{H2O} + P_{CO}K_{CO} + P_{CH4}K_{CH4} \qquad (7)$$

where, σ is the Stefan Boltzmann constant, T is the radiating substance temperature, T_∞ is the ambient temperature and P_k is the partial pressure of the species.

Oppdiff program developed by Lutz et al. [20] is used to solve Eqs. (2)-(5) considering a Lewis number different the unity [22] and a low Mach number. Chemical kinetics is represented by the GRI-Mech 3.0 mechanism which includes 53 species and 325 elementary reactions [23].

3. NUMERICAL PROCEDURE VALIDATION

To validate the numerical procedure, the experimental investigation of Jongmook Lim et al. [24] on opposed flow flame is used. The distribution of the molar fractions of the species is presented in function of the distance between the oxidant and fuel nozzle (L=15 mm in this case). The ambient pressure is P=1 atm, the air temperature is 560 K, the fuel injection temperature is 300 K under a strain rate a=193 s^{-1}. Figure 2(a) represents the consumption of reactants (CH_4, O_2, N_2) which is well predicted relatively to the experimental measures. The molar fractions of major and minor species (H_2, CO, CO_2, NO) in Figures 2(b) and (c) are consistent with the experimental results. the mean error of H_2, CO, CO_2 and NO are 4.70, 12.01, 11.02 and 8.33% respectively (Figure 2(d)).

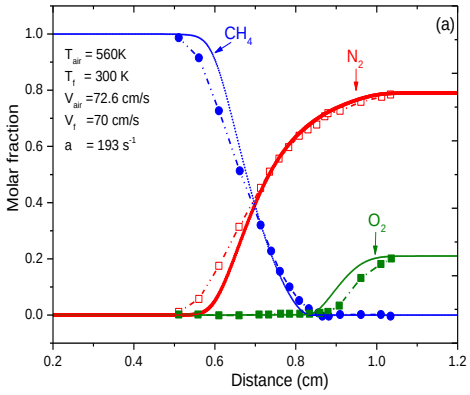

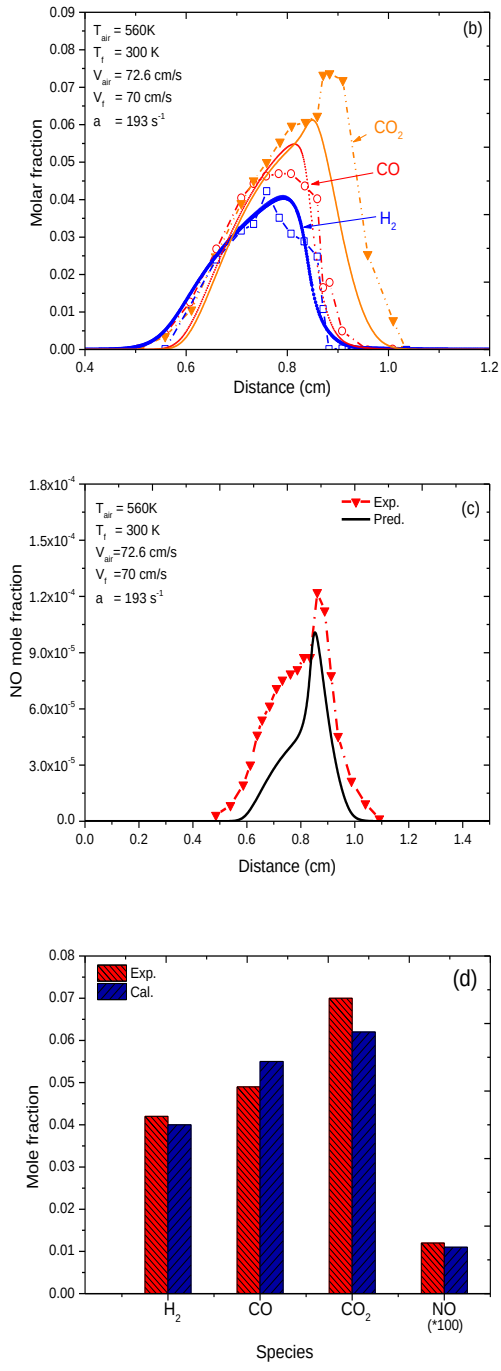

Figure 2. Comparison of measured and calculated values, symbols represent experimental results and lines calculated and mean error

4. RESULTS AND DISCUSSION

4.1 The flame relative temperature

The concept of fractional flame temperature f is used to take into account the radiation of the flame. f is defined as follows [25]:

$$f = \frac{T_{nr} - T_r}{T_{nr}} \qquad (8)$$

where, T_{nr} and T_r denote the adiabatic and radiating flame temperatures respectively. Figure 3 illustrates the evolution of

f in the mixture fraction space for several operating conditions. It is noticed that the enrichment in oxygen and the increase in CO_2 fractions, in the synthetic atmosphere, decrease the value of f (Figure 3(a) and (c)). On one hand, increasing oxygen in the oxidizer, in this case, enhances reaction and adiabatic flame temperature increases, which reduces the flame relative temperature. On the other hand, increasing strain rate, reduces the flame volume and obviously the radiation losses, which reduces the flame relative temperature. When CO_2 volume increase in the mixture Figure 3(b), the relative temperature of the flame increases significantly since CO_2 is a strong source of gaseous radiation [26].

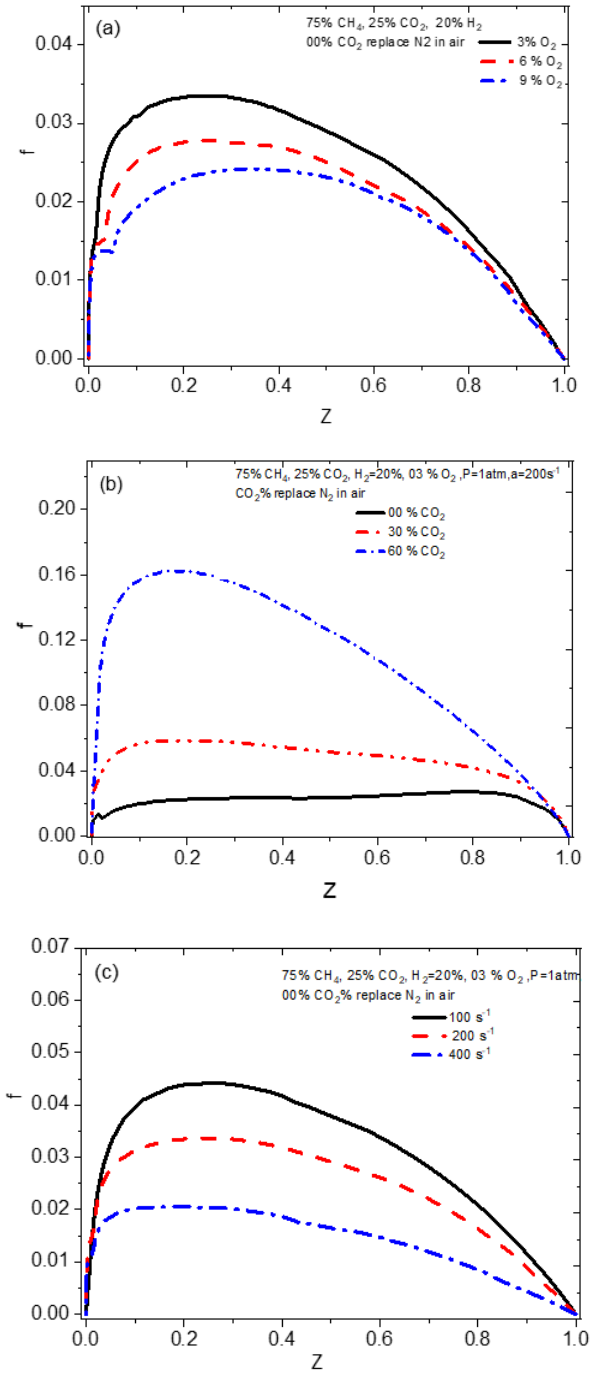

Figure 3. Relative temperature evolution for different values of mole fractions of O_2, CO_2 and strain rate a

4.2 Effects of oxygen enrichment on the flame structure

The Figure 4 shows the flame structure in term of temperature and the species OH, CO, C_2H_2 and NO for different volumetric compositions of the synthetic atmosphere (O_2=3%, 6% and 9% and CO_2=0 and 60%). It is noticed that in the absence of CO_2 in the oxidant mixture, the decrease in oxygen from 9 to 3% induces a reduction in temperature (Figure 3(a)) and a slight shift towards the oxidizer side. Indeed, the maximum temperature falls from 1800 K for 9% of O_2 to 1400 K for 3% of O_2, i.e., a decrease of 22%. Probably, this is the consequence of lack of oxygen which makes the mixture locally rich and by the way the decrease in temperature.

The same behavior is observed when N_2 is replaced by CO_2 (at CO_2=60%) in the oxidizer stream for the same oxygen concentration. In this case the decrease in maximum temperature is about 16% and it is the result of the higher heat capacity of CO_2 compared to N_2. It should be noted that MILD regime is reached at these operating conditions since the difference between maximum flame temperature and oxidant temperature is 600 K, lower than the self-ignition temperature of the fuel mixture which is more than 800 K.

The species profiles in Figure 4 follow the same trend of variation of temperature. There is a reduction in their peak and a shift in profiles towards the oxidizer side. The respective percent diminutions are reported in Table 2.

Table 2. Percentile decrease
BG 75%+20% H_2, 6% O_2, P=1 atm and a=200 s^{-1}

Species	Decrease with 60% CO_2
OH	66.41%
CO	20.31%
C_2H_2	95.28%
NO	99.32%

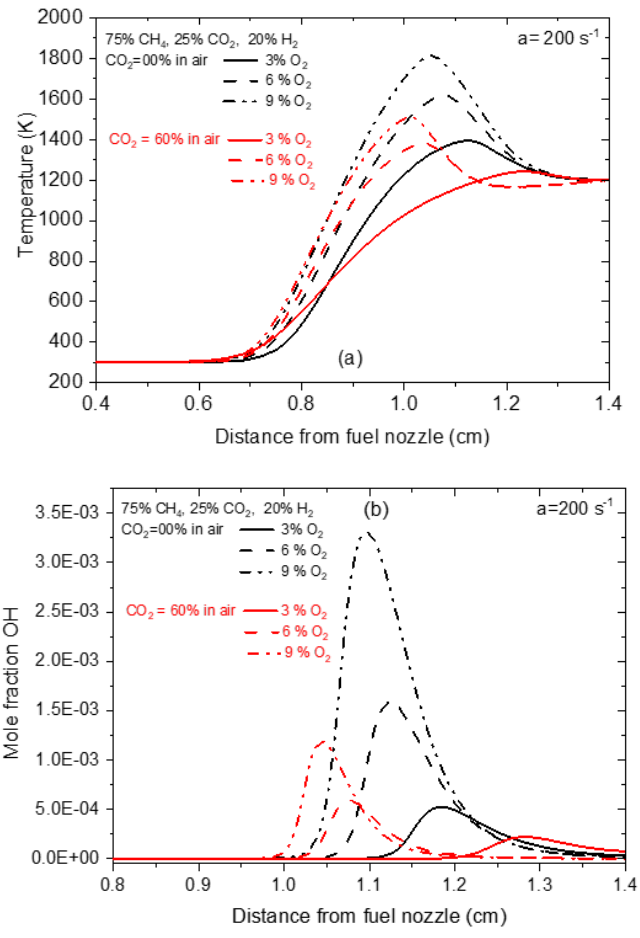

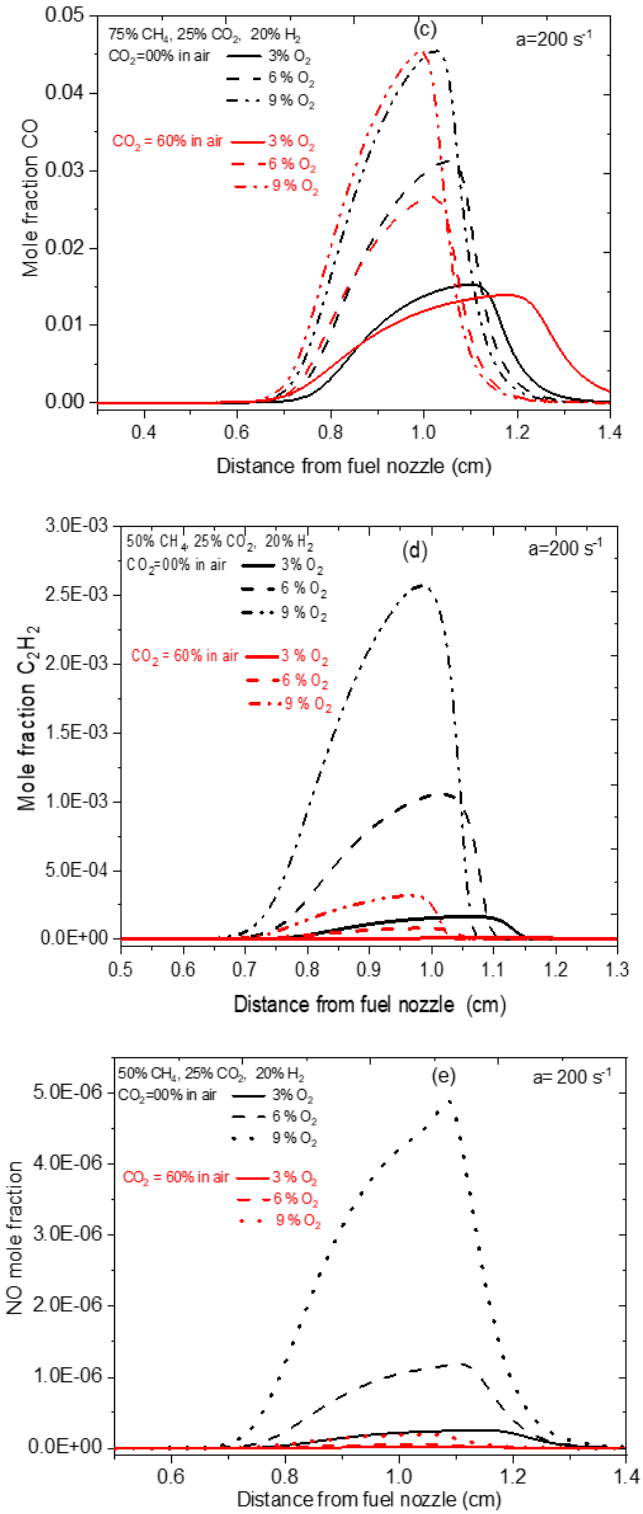

Figure 4. Axial profiles of temperature and molar fractions of OH, CO, C_2H_2, and NO

The C_2H_2 species is a precursor of soot formation [27] which is responsible for the nucleation of soot by these elementary reactions. Increasing the oxygen content as shown in Table 1 induces oxidation of this species. It should be noted that replacing N_2 in the air with CO_2 in the oxidizer stream leads to a very significant reduction in CO, C_2H_2 and NO.

4.3 Oxygen and diluent effects on the maximum temperature and species

The Figure 5 shows the variation of maximum temperature and species (OH, NO and C_2H_2) in function of the CO_2 in the oxidizer stream, for different O_2 contents and strain rate values at atmospheric pressure. It is noticed that the temperature (Figure 5(a)) decreases with the decrease of O_2 and the increase of CO_2 regardless of the value of the strain rate. This is due to the slowdown of the chemical reaction in the O_2 poor atmosphere and also to the high heat capacity of CO_2 compared to N_2. It can also be seen that the decrease in maximum temperature increases with the rate of deformation due to the reduction in residence time. The species considered such as OH (Figure 5(b)) and C_2H_2 (Figure 5(c)) present the same tendency as the temperature. NO is less sensitive to CO_2 than C_2H_2 within the range of the considered strain rate (Figure 5(d)). Indeed, NO vanishes from 30% of CO_2 for O_2 content higher than 3% whatever the value of the strain rate. Also, NO and C_2H_2 formations vanish both at O_2=3% at all the fraction of CO_2 and the strain rate value.

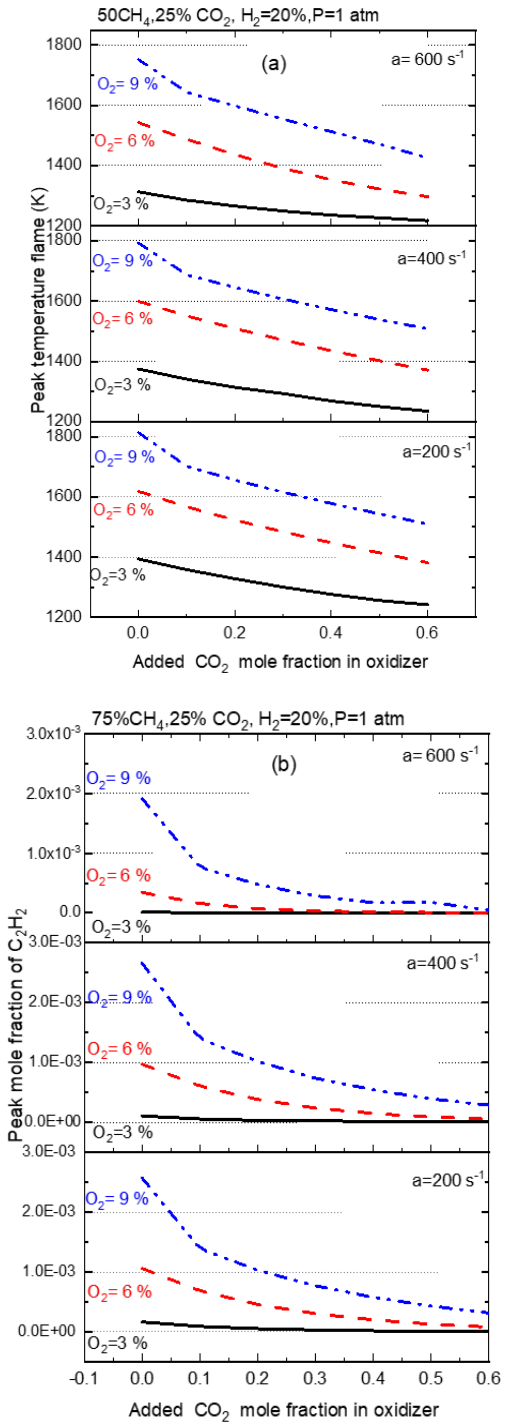

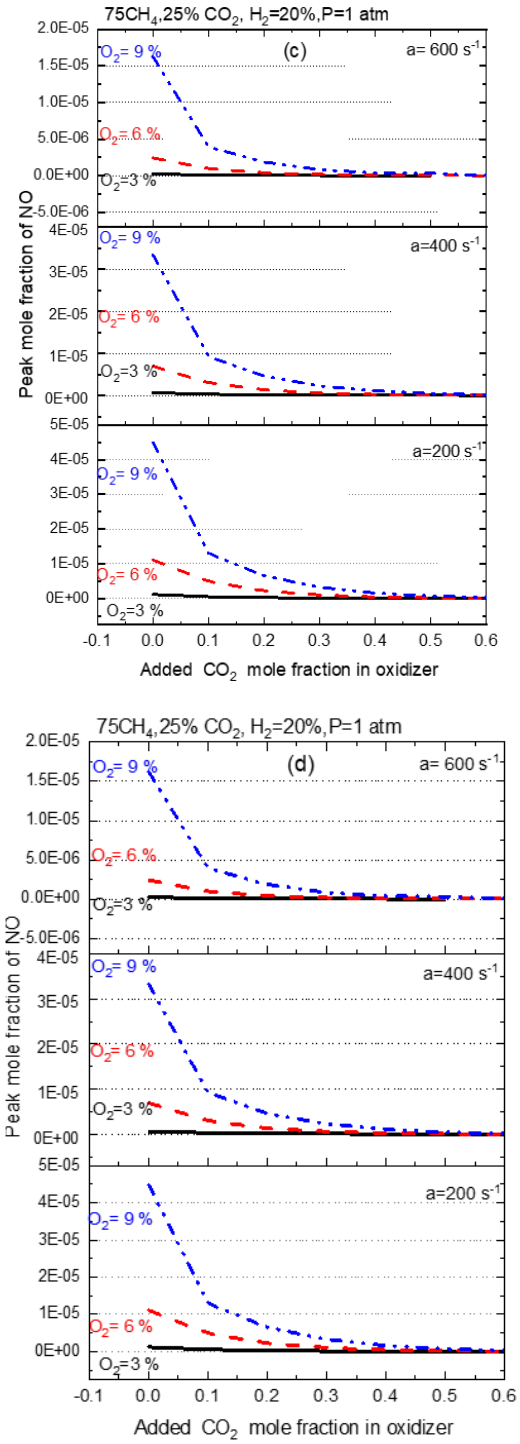

Figure 5. Effects of CO_2, O_2 and strain rate on the variation of maximums: (a) Temperature, molar fractions of (b)OH, (c) C_2H_2, and (d) NO

4.4 The chemical effect of CO_2 added to the oxidizer

This effect is computed at atmospheric pressure and at a strain rate of 200 s^{-1} for an oxygen volume of 3% and 6%, as shown in Figure 6. An inert artificial species F_CO_2, which has properties (transport, radiation and thermochemical) similar to those of CO_2, is introduced to characterize the CO_2 chemical effects on the structure and emissions of the biogas flame. Two computations are achieved. Then, the difference between the flame properties calculated with the species F_CO_2 and CO_2 represent this chemical effect. The Figure 6 (a) shows that, for a given volume of oxygen, CO_2 addition reduces maximal temperature. Also, this effect declines with the O_2 decrease until vanishing at 3% for NO species.

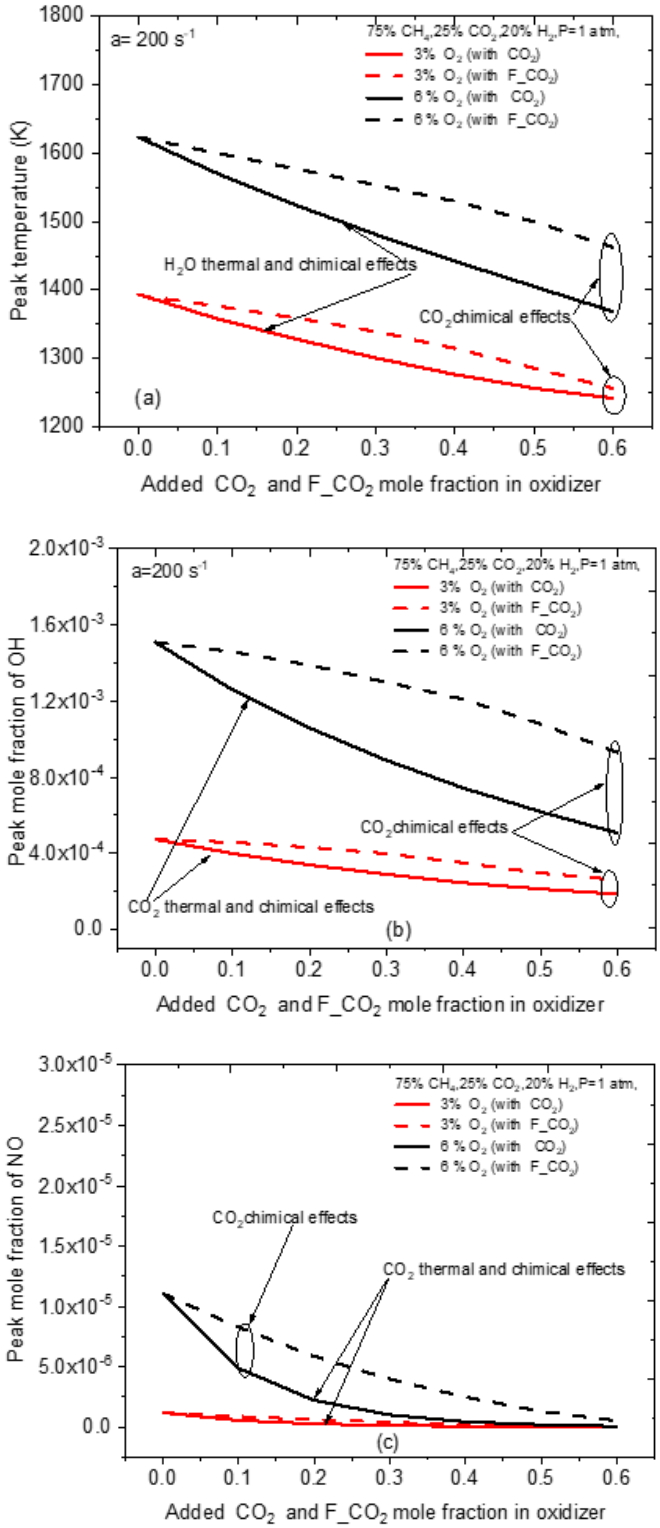

Figure 6. Chemical effect of CO_2 in the oxidizer on the variation of the maximums of: (a) temperature and the molar fractions of (b) OH and (c) NO

In Figure 6(b), CO_2 chemical effect decreases continuously the maximum of OH, especially at 6% of O_2. The low oxygen content in the oxidant reduces considerably the formation of NO. Figure 6(c) depicts that NO peaks are reduced by CO_2 chemical effects and no effect is noticed at 3% of O_2. The chemical effects of the added CO_2 propagate according to the

reaction $H+CO_2=CO+OH$; and $H+O_2=O+OH$ represents the reaction rate index. The consumption of the H radicals is carried out in the step $H+CO_2=CO+OH$. Thus, the reaction $H+O_2=O+OH$ will not take place, this eliminates the main branching chain [28]. It is noted that when hydrogen is added to biogas, the rates of the reactions $H+CO_2=CO+OH$ and $H+O_2=O+OH$ increase increases the temperature relative to the reactivity of the H and OH chain carriers.

5. CONCLUSION

A numerical study of the characteristics of the diffusion flame of hydrogen mixed with biogas (BG75-H_2) in a synthetic atmosphere was carried out. Different compositions of the oxidizer were considered at diverse values of strain rate (200 s^{-1}, 400 s^{-1} and 600 s^{-1}). Moreover, the chemical effect of CO_2 was elucidated. The following conclusions can be drawn out:

The substitution of N_2 by CO_2 decreases the maximum flame temperature significantly. Furthermore, chain-carrying radicals such as OH and pollutants like C_2H_2 and NO, are also reduced independently of the O_2 content and strain. However, NO is found to be less sensitive to CO_2 than C_2H_2. Also, O_2 reduction and CO_2 increase induce a reduction in NO and C_2H_2 productions. In addition, NO and C_2H2 formations vanish both at O_2=3% whatever the values of CO_2 and the strain rate.

The chemical effect of CO_2 is present over the entire strain rate range considered. Whatever the CO_2 values, as long as the O2 concentration is greater than 3%, it leads to a decrease in temperature, OH and NO peaks.

REFERENCES

[1] Izah, S.C., Iyiola, A.O., Yarkwan, B., Richard, G. (2023). Chapter 7 - Impact of air quality as a component of climate change on biodiversity-based ecosystem services. In Visualization Techniques for Climate Change with Machine Learning and Artificial Intelligence, Elsevier, pp. 123-148. https://doi.org/10.1016/B978-0-323-99714-0.00005-4

[2] Won, S.H., Kim, J., Hong, K.J., Cha, M.S., Chung, S.H. (2005). Stabilization mechanism of lifted flame edge in the near field of coflow jets for diluted methane. Proceedings of the Combustion Institute, 30(1): 339-347. https://doi.org/10.1016/j.proci.2004.08.010

[3] Chen, S., Liu, Z., Liu, J., Li, J., Wang, L., Zheng, C. (2010). Analysis of entropy generation in hydrogen-enriched ultra-lean counter-flow methane–air non-premixed combustion. International Journal of Hydrogen Energy, 35(22): 12491-12501. https://doi.org/10.1016/j.ijhydene.2010.08.048

[4] Mameri, A., Tabet, F., Hadef, A. (2017). Numerical investigation of biogas diffusion flames characteristics under several operation conditions in counter-flow configuration with an emphasis on thermal and chemical effects of CO_2 in the fuel mixture. Heat and Mass Transfer, 53: 2701-2710. https://doi.org/10.1007/s00231-017-2017-4

[5] Katsuki, M., Hasegawa, T. (1998). The science and technology of combustion in highly preheated air. Symposium (International) on Combustion, 27(2): 3135-3146. https://doi.org/10.1016/S0082-0784(98)80176-8

[6] De Joannon, M., Sorrentino, G., Cavaliere, A. (2012). MILD combustion in diffusion-controlled regimes of hot diluted fuel. Combustion and Flame, 159(5): 1832-1839. https://doi.org/10.1016/j.combustflame.2012.01.013

[7] Park, J., Kim, S.G., Lee, K.M., Kim, T.K. (2002). Chemical effect of diluents on flame structure and NO emission characteristic in methane-air counterflow diffusion flame. International Journal of Energy Research, 26(13): 1141-1160. https://doi.org/10.1002/er.841

[8] Zhen, H.S., Leung, C.W., Cheung, C.S. (2013). Effects of hydrogen addition on the characteristics of a biogas diffusion flame. International Journal of Hydrogen Energy, 38(16): 6874-6881. https://doi.org/10.1016/j.ijhydene.2013.02.046

[9] Mameri, A., Tabet, F. (2016). Numerical investigation of counter-flow diffusion flame of biogas–hydrogen blends: effects of biogas composition, hydrogen enrichment and scalar dissipation rate on flame structure and emissions. International Journal of Hydrogen Energy, 41(3): 2011-2022. https://doi.org/10.1016/j.ijhydene.2015.11.035

[10] Dally, B.B., Riesmeier, E., Peters, N. (2004). Effect of fuel mixture on moderate and intense low oxygen dilution combustion. Combustion and Flame, 137(4): 418-431. https://doi.org/10.1016/j.combustflame.2004.02.011

[11] Oh, K.C., Shin, H.D. (2006). The effect of oxygen and carbon dioxide concentration on soot formation in non-premixed flames. Fuel, 85(5-6): 615-624. https://doi.org/10.1016/j.fuel.2005.08.018

[12] Chen, S., Zheng, C. (2011). Counterflow diffusion flame of hydrogen-enriched biogas under MILD oxy-fuel condition. International Journal of Hydrogen Energy, 36(23): 15403-15413. https://doi.org/10.1016/j.ijhydene.2011.09.002

[13] Mameri, A., Tabet, F., Hadef, A. (2018). MILD combustion of hydrogenated biogas under several operating conditions in an opposed jet configuration. International Journal of Hydrogen Energy, 43(6): 3566-3576. https://doi.org/10.1016/j.ijhydene.2017.04.273

[14] Lock, A., Briones, A.M., Aggarwal, S.K., Puri, I.K., Hegde, U. (2007). Liftoff and extinction characteristics of fuel-and air-stream-diluted methane–air flames. Combustion and Flame, 149(4): 340-352. https://doi.org/10.1016/j.combustflame.2007.02.007

[15] Takahashi, F., Linteris, G.T., Katta, V.R. (2007). Extinguishment mechanisms of coflow diffusion flames in a cup-burner apparatus. Proceedings of the Combustion Institute, 31(2): 2721-2729. https://doi.org/10.1016/j.proci.2006.08.112

[16] Park, J., Kim, J.S., Chung, J.O., Yun, J.H., Keel, S.I. (2009). Chemical effects of added CO_2 on the extinction characteristics of $H_2/CO/CO_2$ syngas diffusion flames. International Journal of Hydrogen Energy, 34(20): 8756-8762. https://doi.org/10.1016/j.ijhydene.2009.08.046

[17] Amar, H., Abdelbaki, M., Fouzi, T., Zeroual, A. (2018). Effect of the addition of H_2 and H_2O on the polluting species in a counter-flow diffusion flame of biogas in flameless regime. International Journal of Hydrogen Energy, 43(6): 3475-3481. https://doi.org/10.1016/j.ijhydene.2017.11.159

[18] Shu, Z., Dai, C., Li, P., Mi, J. (2018). Nitric oxide of MILD combustion of a methane jet flame in hot oxidizer coflow: Its formations and emissions under H_2O, CO_2 and N_2 dilutions. Fuel, 234: 567-580.

https://doi.org/10.1016/j.fuel.2018.07.057
[19] Seghaier, B.M., Amar, H., Abdelbak, M., Zeroual, A. (2023). The effect of strain rate and the chemical effects of H_2 and CO on the soot formation of ethylene-syngas in opposed jet laminar diffusion flame. International Journal of Heat and Technology, 41(2): 323-331. https://doi.org/10.18280/ijht.410205
[20] Lutz, A.E., Kee, R.J., Grcar, J.F., Rupley, F.M. (1997). OPPDIF: A Fortran program for computing opposed-flow diffusion flames (No. SAND-96-8243). Sandia National Lab. (SNL-CA), Livermore, CA (United States). https://doi.org/10.2172/568983
[21] Ning, D., Fan, A., Yao, H. (2017). Effects of fuel composition and strain rate on NO emission of premixed counter-flow H_2/CO/air flames. International Journal of Hydrogen Energy, 42(15): 10466-10474. https://doi.org/10.1016/j.ijhydene.2016.12.059
[22] Park, J., Lee, D.H., Yoon, S.H., Vu, T.M., Yun, J.H., Keel, S.I. (2009). Effects of Lewis number and preferential diffusion on flame characteristics in 80% H_2/20% CO syngas counterflow diffusion flames diluted with He and Ar. International Journal of Hydrogen Energy, 34(3): 1578-1584. https://doi.org/10.1016/j.ijhydene.2008.11.087
[23] Smith, G.P., Golden, D.M., Frenklach, M., Moriarty, N.W., Eiteneer, B., Goldenberg, M. GRI Mech-3.0. http://www.me.berkeley.edu/grimech/, accessed on Jan. 27, 2022.
[24] Lim, J., Gore, J., Viskanta, R. (2000). A study of the effects of air preheat on the structure of methane/air counterflow diffusion flames. Combustion and flame, 121(1-2): 262-274. https://doi.org/10.1016/S0010-2180(99)00137-6
[25] Zouagri, R., Mameri, A., Tabet, F., Hadef, A. (2020). Characterization of the combustion of the mixtures biogas-syngas at high strain rates. Fuel, 271: 117580. https://doi.org/10.1016/j.fuel.2020.117580
[26] Xu, H., Liu, F., Sun, S., Zhao, Y., Meng, S., Tang, W. (2017). Effects of H_2O and CO_2 diluted oxidizer on the structure and shape of laminar coflow syngas diffusion flames. Combustion and Flame, 177: 67-78. https://doi.org/10.1016/j.combustflame.2016.12.001
[27] Park, S.H., Lee, K.M., Hwang, C.H. (2011). Effects of hydrogen addition on soot formation and oxidation in laminar premixed C_2H_2/air flames. International Journal of Hydrogen Energy, 36(15): 9304-9311. https://doi.org/10.1016/j.ijhydene.2011.05.031
[28] Liu, D., Santner, J., Togbé, C., Felsmann, D., Koppmann, J., Lackner, A., Yang, X., Shen, X., Ju, Y., Kohse-Höinghaus, K. (2013). Flame structure and kinetic studies of carbon dioxide-diluted dimethyl ether flames at reduced and elevated pressures. Combustion and Flame, 160(12): 2654-2668. https://doi.org/10.1016/j.combustflame.2013.06.032

NOMENCLATURE

a	strain rate, s^{-1}
Cp	specific heat, J kg^{-1} K^{-1}
D_Z	diffusion coefficient, m^2s^{-1}
h_i	enthalpy of species i, J kg^{-1}
N_k	Number of moles of species k, moles
f	relative temperature
P	operating pressure, atm
$\dot{q}_r$	radiative heat loss, W m^{-2}
T_r	Temperatures without radiation, K
T_{nr}	Temperatures with radiation, K
T	Local ambient temperature, K
T_∞	Temperature of the radiating substance, K
Y_F	Feed stream mass fraction of the fuel
Y_O	Feed stream mass fraction of the oxygen

Greek symbols

λ	thermal conductivity, W $m^{-1}K^{-1}$
ρ	density, kg m^{-3}
σ	steffan-boltzmann constant, 5.669 x 10^{-8} W $m^{-2}K^{-4}$
u_O	Velocity of the oxidant, $cm.s^{-1}$
u_F	Velocity of the fuel, $cm.s^{-1}$